



This is a repository copy of *Investigating rolling as mechanism for humeral fractures in non-ambulant infants : a preliminary finite element study.*

White Rose Research Online URL for this paper:
<http://eprints.whiterose.ac.uk/151913/>

Version: Published Version

Article:

Altai, Z., Viceconti, M. orcid.org/0000-0002-2293-1530, Li, X. et al. (1 more author) (2019) Investigating rolling as mechanism for humeral fractures in non-ambulant infants : a preliminary finite element study. *Clinical Radiology*. ISSN 0009-9260

<https://doi.org/10.1016/j.crad.2019.08.026>

Reuse

This article is distributed under the terms of the Creative Commons Attribution-NonCommercial-NoDerivs (CC BY-NC-ND) licence. This licence only allows you to download this work and share it with others as long as you credit the authors, but you can't change the article in any way or use it commercially. More information and the full terms of the licence here: <https://creativecommons.org/licenses/>

Takedown

If you consider content in White Rose Research Online to be in breach of UK law, please notify us by emailing eprints@whiterose.ac.uk including the URL of the record and the reason for the withdrawal request.

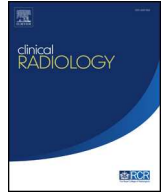


eprints@whiterose.ac.uk
<https://eprints.whiterose.ac.uk/>



Contents lists available at ScienceDirect

Clinical Radiology

journal homepage: www.clinicalradiologyonline.net

Investigating rolling as mechanism for humeral fractures in non-ambulant infants: a preliminary finite element study[☆]

Z. Altai^{a,b}, M. Viceconti^{a,b,1}, X. Li^{a,b,*}, A.C. Offiah^{b,c}

^aDepartment of Mechanical Engineering, University of Sheffield, UK

^bInsigneo Institute for in silico Medicine, University of Sheffield, UK

^cDepartment of Oncology and Metabolism, University of Sheffield, UK

ARTICLE INFORMATION

Article history:

Received 4 June 2019

Accepted 29 August 2019

AIM: To use personalised computed tomography (CT)-based finite element models to quantitatively investigate the likelihood of self-inflicted humeral fracture in non-ambulant infants secondary to rolling.

MATERIALS AND METHODS: Three whole-body post-mortem CT examinations of children at the age of rolling (two 4-month-old and one 6-month-old) were used. The mechanical moment needed by each infant to perform a rolling manoeuvre was calculated and applied to the finite element model in order to simulate spontaneous rolling from the prone to the supine position.

RESULTS: The maximum predicted strains were found to be substantially lower (with a difference of >80%) than the elastic limit of the bone.

CONCLUSION: Results of this study challenge the plausibility of self-inflicted humeral fracture caused by rolling in non-ambulant infants and indicate that it is unlikely for a humeral fracture to result from this mechanism without the assistance of an external force.

© 2019 The Royal College of Radiologists. Published by Elsevier Ltd. This is an open access article under the CC BY-NC-ND license (<http://creativecommons.org/licenses/by-nc-nd/4.0/>).

Introduction

It is uncertain whether non-ambulant infants can sustain humeral fractures when rolling, without the addition of an

external force. In 1996, a possible accidental mechanism of humeral fractures in infants at the age of rolling was reported.¹ It was proposed that a humeral fracture might occur when an infant rolled from prone to supine assisted by another person (i.e., with the addition of an external force). Two cases of humeral fracture were reported; a 5-month-old boy (Case 1) and a 3-month-old girl (Case 2). In Case 1, the injury event was fortuitously videotaped. The video showed the child lying in a prone position, with one arm extended away from his body. The sound of a fracture was heard as the child was rolled over to the supine position by his two-year-old sister. According to medical records, the child sustained an oblique spiral fracture of his humeral diaphysis. After a review of the videotape and family

[☆] The full set of results can be freely downloaded (<https://doi.org/10.15131/shef.data.7301591>). Please contact the corresponding author for further information on data access policies.

* Guarantor and correspondent: X. Li, Insigneo Institute for in silico Medicine, The Pam Liversidge Building, The Sir Robert Hadfield Building, Mappin Street, Sheffield S1 3JD, UK. Tel.: +44 114 222 7786.

E-mail address: xinshan.li@sheffield.ac.uk (X. Li).

¹ Present address: Department of Industrial Engineering, Alma Mater Studiorum, University of Bologna, IT Medical Technology Lab, IRCCS Istituto Ortopedico Rizzoli, Bologna, IT.

evaluation by a multidisciplinary team, the injury was considered unintentional. In Case 2, the mechanism of injury as described by father using a doll was videotaped. The father was helping his daughter to roll onto her back (i.e., from prone to supine), her arm became trapped under her back and the fracture occurred. An oblique spiral fracture of the humeral diaphysis was also reported in this case. By reviewing the videotape of father demonstrating the event, a multidisciplinary team concluded that he did not intentionally cause the injury.

In a second, more recent study, seven cases of humeral fracture were reported and described as possible “accidental injuries”, secondary to the above Hymel mechanism.² The infants were all aged between 4 and 7-months old; however, unlike the Hymel report,¹ there was no known external force acting on the body during the roll. Furthermore, there was no video evidence or witness available to ascertain the injury mechanism. It should also be noted that this study included cases of children rolling in both directions (prone to supine and supine to prone), whereas neither of the Hymel cases was rolling from supine to prone. Somers and his colleagues recognised these inconsistencies and were successful in their overarching goal of fuelling debate in the clinical radiology community.^{3,4}

The detection of child abuse is faced with numerous challenges, a major one being the absent or even misleading history given by the caretaker(s) when explaining the cause of the injury. Furthermore, very little information is known about how paediatric bones fracture under various loads, or their injury tolerance. For these reasons, clinicians mainly rely on their experience. Very recently, computed tomography (CT)-based finite element modelling, a widely used approach to study adult bones,^{5–7} has been successfully used to study the mechanical response of children’s bones under external loads.^{8–12} An important factor in fracture mechanisms that can be readily investigated using finite element models is the comparison between the physical force acting on the bone and the predicted failure (fracture) force.

The aim of this study was to investigate the possibility of self-inflicted humeral fractures in infants while rolling from prone to supine (as suggested by Somer’s study²) using a CT-based finite element modelling approach, considering both personalised geometry and bone material properties.

Material and methods

Post-mortem CT examinations of three infants performed at Sheffield Children’s Hospital were used. The three cases used in this paper form part of a larger pilot study at which ethics was approved to use the CT scans for research purposes.⁸ The study was registered with the local Research & Development Department (registration number CA11024).

One of these infants had an injured right humerus; therefore, the left humerus of each of the three children was segmented and used for this study.

Finite element model generation

The three-dimensional (3D) geometry of each humerus was segmented using ITKsnap. The segmented geometries were then automatically meshed in ICEM CFD 15.0 (Ansys INC., PA, USA) with 10-node tetrahedral elements. The mechanical properties of bone tissue vary from point to point, primarily as a function of its microporosity and degree of mineralisation. Heterogeneous material properties (e.g., bone density and modulus of elasticity) were estimated from the CT scan and mapped to the finite element model following a well-validated material-mapping procedure (Bonemat v3, Rizzoli Institute).^{13–15} This procedure has previously been used for paediatric bone, details were described in Li *et al.* (2015) and Altai *et al.* (2018).^{8,9} Mesh convergence analysis was conducted and an anatomical reference system was defined following the same procedure used in Altai *et al.* (2018).⁹

Displacement boundary conditions

According to the hypothesis described by Hymel,¹ the infant’s arm is trapped underneath the trunk. Fig 1 shows a schematic drawing of three stages passed during the manoeuvre from prone to supine. In position (a), the infant is lying on the abdomen (i.e. prone position with $\varphi = 0$), where φ is the angle between the trunk and the lying surface. The infant then uses one arm to push against his/her body weight and starts to roll. At the intermediate position (b), the infant’s trunk is perpendicular to the floor ($\varphi = \pi/2$), where the arm may be trapped between the body and the floor. Because of the minimal strength of the abdominal muscles of young infants, flipping back to the starting position would be difficult. Therefore, the infant will continue to roll to position (c) with ($\varphi = \pi$), at this point and because of the limited movement of the shoulder-scapula joint, the arm remains trapped underneath the body, leading to a self-inflicted humeral fracture.

The boundary conditions in the computer model were chosen to reflect the later stage (from b to c) of the above manoeuvre. Fig 2 shows the representative finite element model in which the proximal and distal ends of the mineralised humerus were connected to the centre of the proximal and distal ossification centres (represented by pilot nodes) using multi-point constraint (MPC) elements. The MPC elements related all degrees of freedom of the nodes at proximal and distal ends of the humerus to the pilot nodes. The pilot nodes also allowed rotational degree of freedoms to be specified, where the humerus was allowed to rotate around the pilot nodes representing the ossification centre. Boundary constraints are detailed in Fig 2 and assigned to the model as follows: the displacements of the distal pilot node were free along the parallel direction to the body centre line (x -axis) and fixed in both y and z directions. In other words, the arm was assumed to be fixed between the trunk and the underlying surface (medial–lateral plane of the humerus). Any flexion or extension (anterior–posterior plane of the humerus) was prevented. The arm was assumed to be fixed while the body of the child

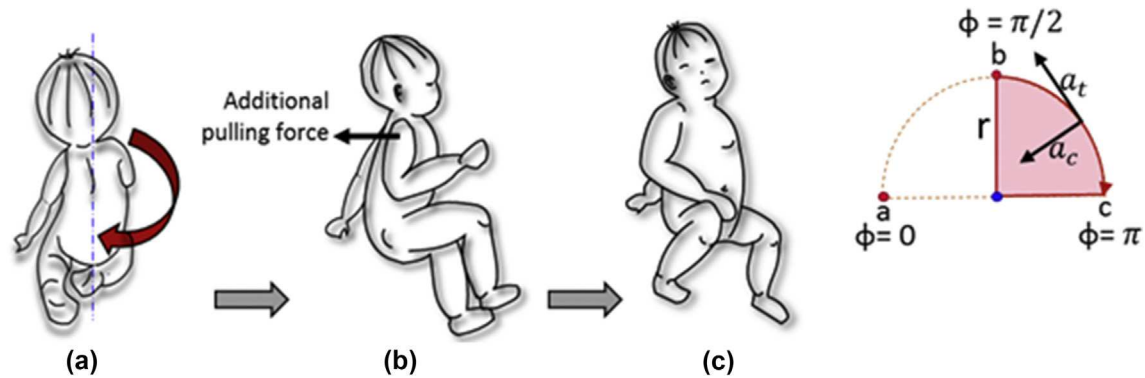


Figure 1 Three stages of an infant rolling from prone to supine. Position (a) is the starting position (prone) when the infant is lying on his/her abdomen. Position (b) is when the trunk is perpendicular to the floor, the black arrow represents an additional external force which might act on the arm during rolling, such as pulling the infant or forcing the rolling manoeuvrer. And position (c) is the final position when the infant is lying on his/her back (supine) – note the infant’s arm trapped under his/her body.

was rotating around the shoulder joint; hence rotation of the distal pilot node was not allowed around the long axis of the humerus (or x -axis). The displacement of the proximal pilot node was fixed in the x direction to mimic the effect of the shoulder joint (all other degrees of freedom were unconstrained). This boundary condition was chosen in order to minimise the constrained degrees of freedom while avoiding rigid body motion of the model.

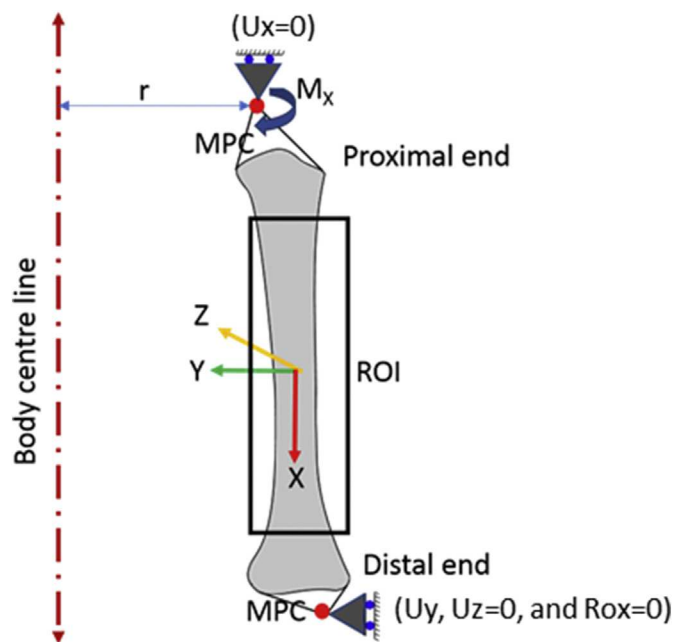


Figure 2 Finite element model of the humerus. Proximal and distal ends were connected to the pilot nodes (red nodes) by Multi Point Constraints elements. The pilot nodes were located at the centre of the proximal and distal ossifications. A rotational moment (M_x) was applied at the proximal end representing the rotation around the centre of the shoulder joint. The distance between the body centre line and the proximal ossification centre is the moment arm indicated by r . ROI is the region of interest as highlighted by the black rectangle. U_x , U_y , and U_z are the displacement degrees of freedom in the X , Y and Z axis respectively. R_{ox} is the rotational degree of freedom around the X axis.

Force boundary conditions

Given the same rolling direction (from prone to supine), the main difference between Hymel and Somers’ study is the presence of evidenced external force during the manoeuvre. Video evidence reported in Hymel *et al.* (1996) suggested that an external force could lead to humeral fractures, whereas Somers *et al.* (2014) suggested that fracture is possible without an applied external force.

The study reported here first focused on reproducing the Somers’ loading scenario, whereby the rotational moment needed by each infant to roll was calculated based on the total body mass of the child and the acceleration needed to complete a rotation from position b to position c, as shown in Fig 2. Adopting a “worst case scenario” model, it was assumed that the total body mass of each infant would contribute to the rotation and that the time needed to roll from position b to position c was 0.3 seconds. The moment arm was considered as the distance between the proximal ossification centre and the body centre line of the infant. The moment was applied at the proximal pilot node around the long axis of the humerus. All variables used as input to the finite element model are summarised in Table 2.

During the rolling manoeuvre and when the body is directly on top of the arm, the arm may be held in a variety of different angles with respect to the trunk; however, because of the complexity of the shoulder–scapula joint, the motion of the arm is limited in this position. The maximum angle in which the arm can move towards the back of the body is 45° in horizontal extension and 60° in vertical extension for adults.¹⁶ Assuming a similar range for very young children, these values were assigned in the simulation as the maximum angles by which the arm could reach behind the body. Sixteen orientations were therefore simulated by incrementing the angle by 15° and 20° in horizontal and vertical extensions, respectively, as shown in Fig 3.

Once Somers’ scenario has been set up, it is relatively straightforward to estimate the effect of an applied external force during the manoeuvre. In order to estimate the magnitude of the required external force to cause fracture,

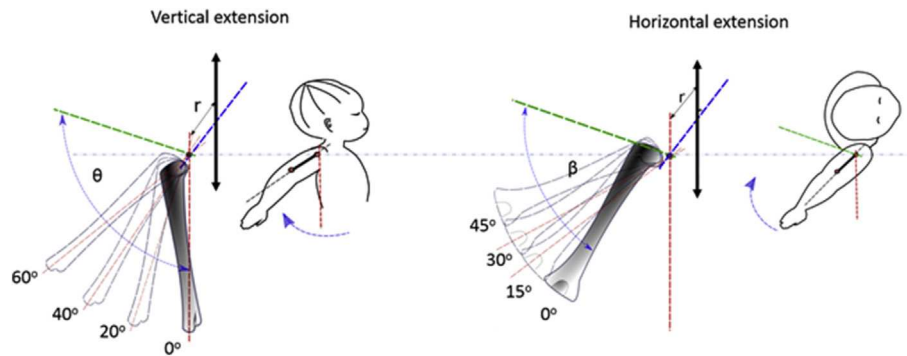


Figure 3 Sixteen simulated orientations of the humeral finite element model. The vertical angle (θ) was incremented by 20 degrees while the horizontal angle (β) was incremented by 15 degrees. The centre line of the body is indicated by the bold double-headed arrows.

the force required to elevate the strain to failure threshold was estimated for each of the three subjects modelled here. This force was assumed to be acting parallel to the lying surface, and orthogonal to the infant trunk. The location of force application was assumed to be the free arm Fig 3b. Therefore, the moment arm in this case was taken as the distance between the right and left proximal humeral ossification centres (i.e. shoulder width). In order to estimate the minimum required external force, the extreme angles of the trapped arm were investigated.

All simulations were run in ANSYS APDL and solved using the preconditioned conjugate gradient-iterative solver (PCG) with a tolerance value of 1E-8.

Post-processing of the principal strains

Both the first (tension) and third (compression) principal strains were evaluated for all the nodes within the region of interest, which is highlighted by the black rectangle in Fig 2. The peak principal strains were extracted from the finite element models under each of the 16 simulated orientations. Among these, the maximum and minimum predicted strains were found and compared with the tensile and compressive elastic limits of human bone (0.73% in tension and 1.04% in compression).¹⁷

Results

The morphological parameters of the humeri show that there is some variation in humeral development within the selected age range (Table 1). Patient 2 generally had a higher modulus of elasticity across the humerus in comparison with the other two patients. This patient had a comparably lower body mass percentile but a higher height percentile, indicating this to be a relatively tall and slim child; however, there was no direct explanation for the higher modulus of elasticity. The distribution of the modulus of elasticity of the three patients is shown in Fig 4. The moment needed for the rolling manoeuvre in patient 2 was much higher (66%) than in patient 1.

The results of this study show that the highest predicted strains are substantially lower, at around 20% of the predicted elastic limit of the three bones evaluated. Fig 5 shows the predicted peak strains (first and third principal strains) of the humerus for all three patients under each orientation. For all three patients, the highest first and third principal strain values were both found when the humerus was located at the extreme angles relative to the body.

If external forces were to be considered in the model, the required external forces to fracture the humerus was predicted at 10.5, 22.5, and 21.5 N for patient 1, patient 2 and

Table 1
Demographics of the infants recruited to this study.

Patient No.	Gender	Age (months)	Body mass (kg)/percentile	Hight (cm)/percentile	Humeral length (cm)	E_x (GPa)	Cause of death
1	M	4	3.85/<2nd	60/9th	8.45	10.66	SIDS
2	F	4	5.79/<9th	65/91st	9.32	15.15	SUDI
3	M	6	7.03/25th	69/50th	9.96	13.26	SIDS

Humeral length was estimated from the CT examinations as the distance between the proximal and the distal ossification centres. The maximum modulus of elasticity was estimated from the measured Hounsfield units of the CT scans.^{8,9}
M, male; F, female; E_x , modulus of elasticity of the linear elastic model; SIDS, sudden infant death syndrome; SUDI, sudden unexpected death in infancy.

Table 2
Variables used in the finite element model of the humerus for the three patients.

Patient no.	Body mass (kg)	Angular displacement (rad)	Time (s)	Moment arm (r) (mm)	Tangential acceleration (m/s^2)	Applied moment (M_x) (Nm)
1	3.85	$\pi/2$	0.3	47.49	0.83	0.15
2	5.79	$\pi/2$	0.3	66.22	1.15	0.44
3	7.03	$\pi/2$	0.3	67.20	1.17	0.55

M_x , moment applied to the finite element model.

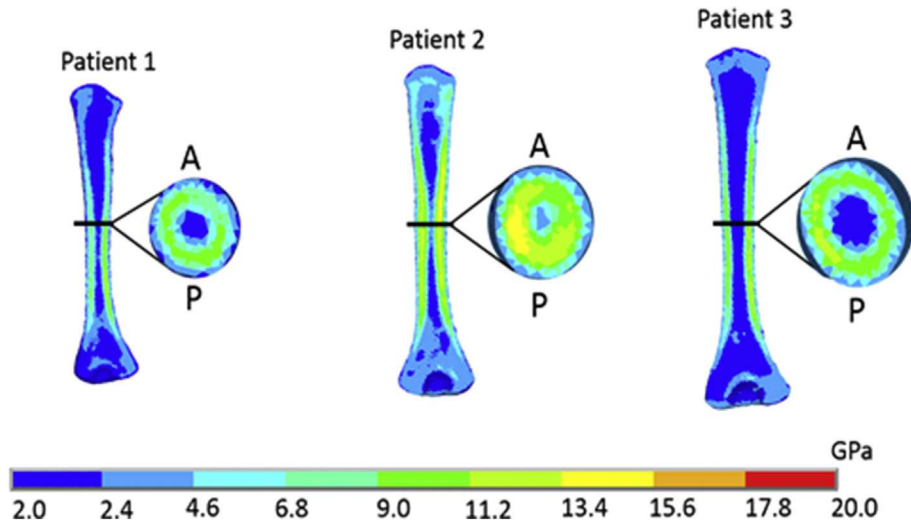


Figure 4 Distribution of the modulus of elasticity (GPa) across the humerus, in the frontal and transverse planes for the three patients. A, anterior; P, posterior.

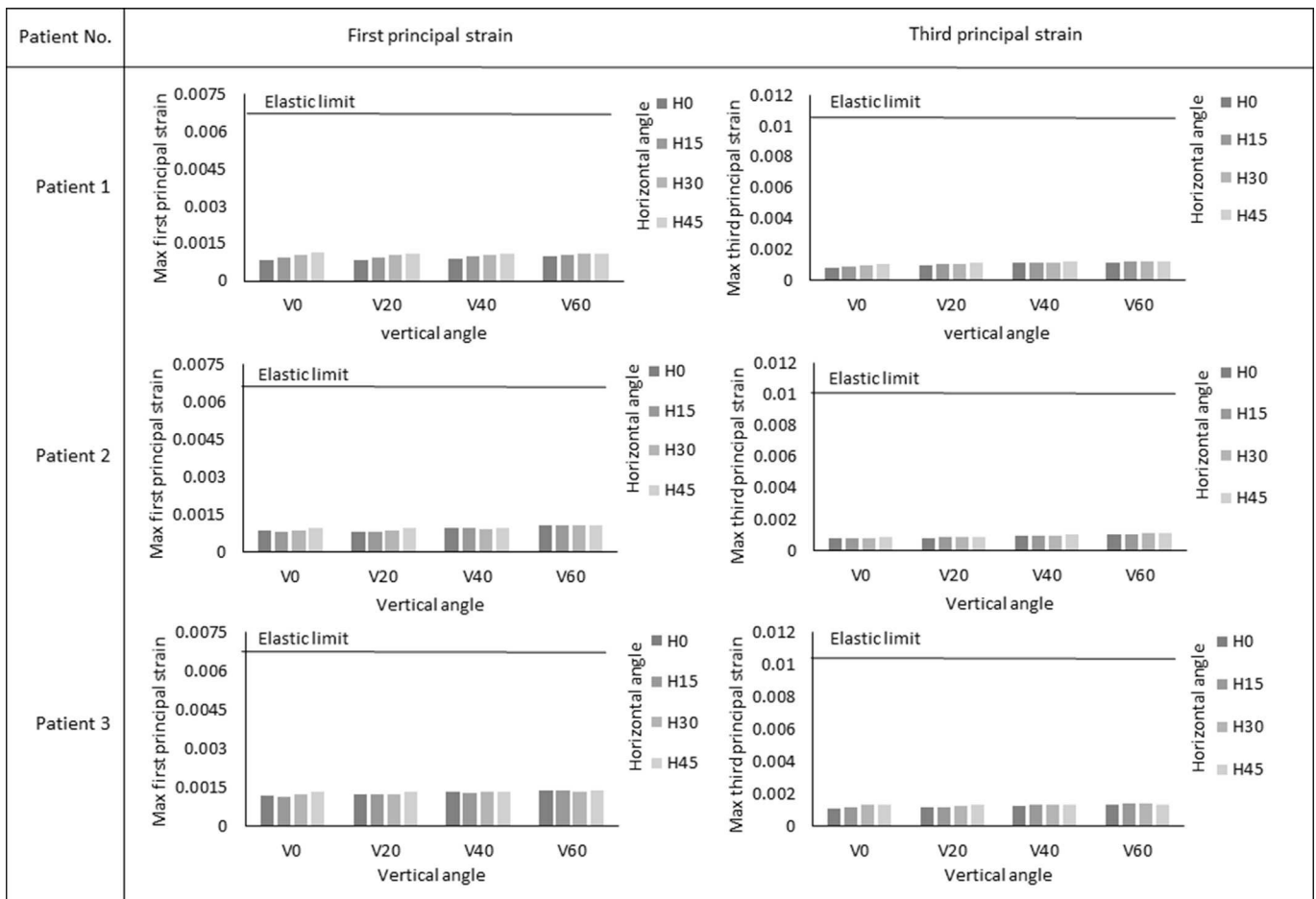


Figure 5 Maximum (first) and minimum (third) principal strains under various orientations of the humerus for the three patients. Sixteen different positions of the humerus (with respect to the body) were simulated. Vertical extension angles ranged from 0° to 60°, with a 20° increment. Horizontal extension angles ranged from 0° to 45°, with a 15° increment. V represents the vertical extension angle, and H represents the horizontal extension angle.

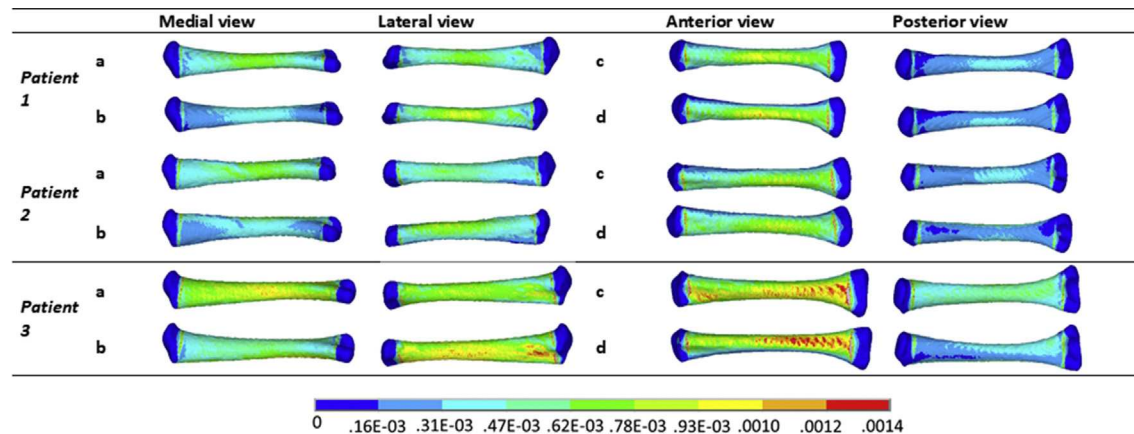


Figure 6 Distribution of the first principal strains (maximum tension) over the humerus for Patients 1, 2 and 3. Four selected orientation scenarios are illustrated: (a) neutral position, (b) 45° horizontal extension with 0° vertical extension, (c) 60° vertical extension with 0° horizontal extension, and (d) a combination of both extreme angles.

patient 3, respectively, under the extreme angles of the trapped arm.

Fig 6 shows the distribution of the first principal strains in the three patients under a few combinations of these extreme angles: (a) neutral position, (b) horizontal extension at 45° (with 0° in vertical extension), (c) vertical extension at 60° (with 0° in horizontal extension), and (d) a combination of both extreme angles. The highest strains were located at the medial side of the humeral shaft when the arm was in the neutral position (scenario a, the body is directly on top of the left arm). This moved to the lateral side of the shaft when the arm was extended horizontally in scenario b. In both scenarios c and d, the highest strains were found at the anterior side of the humerus.

Discussion

The results of this study indicate that the highest predicted strains are substantially lower at around 20% of the predicted elastic limit of human bone.

The aim of the present study was to investigate the likelihood of an infant self-inflicting a humeral fracture while rolling from prone to supine using a CT finite element modelling approach. The case of rolling from supine to prone was not considered, mainly because in this position, the arm is within its normal range of motion, unrestricted by the trunk, in contrast to when the infant rolls from supine to prone.⁴

Care was taken to select infants who were around the age of rolling; two were 4-months old and one was 6-months old (Table 1). The Centre for Disease Control and Prevention Milestone Checklist states most babies when lying on their tummy can push up to their elbows by the end of 4 months and are able to roll from front to back and from back to front by the end of 6 months.

The modelled results in this small sample suggests that rolling over does not generate sufficient force to reach the fracture limit of the infant humerus, while rolling over from front to back without an external force. These results support the arguments of Rosado (2014)

and Jenney (2014).^{3,4} Rosado³ pointed out that it is very doubtful that an infant who can hardly carry his/her own body weight against gravity will have sufficient strength to overcome the failure limit of the humerus. Jenny,⁴ however, claimed that it is difficult to draw a clear conclusion on the likelihood of self-inflicted humeral fracture caused by rolling because the range of bone strength of healthy infants is yet unknown. Since that paper, data have been published on the injury tolerance of infant bones,^{8,9} which coupled with the present findings supports Rosado's opinion that the mechanism is unlikely to cause humeral fractures.

The highest strains were predicted at either the middle or towards the distal end of the humeral diaphysis. This means a fracture would occur at these locations if the bone was to fail under the predicted loads in this study. This is consistent with the location of the fractures reported by Hymel and Somers.^{1,2}

Unsurprisingly, the lowest strains were predicted under the neutral orientation of the humerus for all three patients, whereas the highest strains were all predicted under the extreme angles (either vertical or horizontal extensions or a combination of the two angles). This suggests that bending or extending the arm towards the physical limit would put substantial strains on the arm. The current model indicates that the loading moment produced by the body mass of an infant is not high enough to fracture the bone; however, it is possible for fracture to occur with a sufficient amount of external force.

The current results show that the external pulling force required to fracture the bone during the Hymel manoeuvre is within the normal range that can be exerted by man.¹⁸ This force is relatively small, between 10 and 20 N (equivalent to lifting a 1–2 kg mass or a 1–2 l bottle of milk), and could arise from another person pulling the infant (as reported in Hymel's study), friction, or entanglement with surrounding objects (such as bedding). Because the moment arm (trunk width) is longer than the humerus, this would allow even a toddler to cause fracture by "pulling" the infant. Indeed, this is confirmed by Case 1 presented in

Hymel's report, where a 2-year-old sister rolled her brother over causing his humeral fracture to occur.

In the current study, the maximum angle through which the child's arm could move towards the back of the body was assumed to be in a similar range to adults: 45° in horizontal extension and 60° in vertical extension.¹⁶ This may not be appropriate as children are usually more flexible than adults. The current results show that the predicted strain values increase by 30% when the angle reaches the extreme limit with no more than a 10% increase with each increment. Even if an extension angle of 90° is considered (which is highly unlikely as distortion of the shoulder joint would occur), the predicted strains would still be far below the elastic limit.

There are a number of potential limitations to be addressed. First, only a small number of infants (three) were simulated; however, the maximum forces were so substantially below those required to fracture the humeri of each child, that increasing study numbers without changing the model assumptions is unlikely to make a huge difference to the reported outcomes. This should however be tested. Secondly, due to a lack of input data in the literature, a number of assumptions were made in developing the finite element models. Specifically, the time taken by an infant to complete a rolling manoeuvre and the portion of the body mass contributing to the rolling motion are unknown. Consequently, a worst-case scenario was chosen. The minimum time to complete a roll used to calculate the accelerations was estimated by reviewing representative videos^{19,20} of infants rolling from prone to supine, this ranged from 0.3 to 0.7 seconds. To account for the worst-case scenario, the lower bound value of 0.3 seconds was used in the present model. Similarly, it is reasonable to assume that the entire body mass of the child (e.g., the head) does not contribute to the roll. Nevertheless, to simulate the worst-case scenario, the whole-body mass was considered in the model to calculate the required moment for each child. These assumptions are likely to provide an overestimation of the moment and further reduce the likelihood of this being a mechanism for humeral fractures in the non-ambulant infant.

Furthermore, cartilage, overlying soft tissues, or the increased flexibility of infant (compared to adult bone) was not accounted for in the current study; all of these would further reduce the likelihood of self-inflicted humeral fractures in infants from rolling. Future work should also aim at establishing more accurate boundary conditions for the rolling manoeuvre. This needs to be combined with more accurate calculation of the loads acting on the humerus during rolling from the prone to supine position. Repeated rolling might also occur when infants try to master the manoeuvre. The amount of force generated by this cyclic motion could outweigh a "1 l bottle of milk" and this scenario requires further investigation. Some input data could potentially be generated by monitoring the motion of a rolling infant using motion sensors, such as those used in adults.^{21–24}

Another limitation is the use of maximum strain criterion instead of any shear criterion although the predominant load for the rolling scenario is torsion. This is mainly because of the limited available data in the literature for bone failure criteria. Therefore, the conventional principal strain threshold was used.^{8,9}

A further limitation is that bone biopsy was not performed, and underlying bone disease could not be completely excluded; however, at the authors' institution, routine post-mortem investigation of all infants dying suddenly and unexpectedly, consists of a full skeletal survey or anteroposterior and lateral "babygrams" (depending on size) and conventional autopsy. The radiographs of the three infants recruited to this study were reported as normal by experienced consultant radiologists as part of their routine clinical work. Both the radiographs and post-mortem CT examinations were further reported as normal by a radiologist during the selection process for this study. Following their full routine conventional autopsies (which includes measurement of serum vitamin D and rib histology), causes of death were concluded to be sudden infant death syndrome (SIDS) or sudden unexpected death in infancy (SUDI) as reported in Table 1. Therefore, as far as possible, any underlying bone disorder was eliminated. The possibility of a hitherto unrecognised bone disorder is minimal, but cannot be completely excluded.

Validation of this and similar models remains difficult. One possible solution is to use an instrumented test dummy to quantify the force subjected to the humerus for such injuries and compare against model prediction. Such dummies have been used in the past to investigate paediatric injury risk, such as falling from a short distance^{25,26} and playground accidents.²⁷

It is worth noting that all currently available dynamic models have been developed to simulate adult injuries. Information on humeral and other fractures in infants, including fracture types, patterns, and mechanisms should be collected. Such data will help to inform future finite element modelling studies, thus allowing firmer conclusions to be reached in cases of suspected inflicted injury in children.

In conclusion, the results of the present study show that, in non-ambulant infants, rolling from prone to supine without an applied external force does not generate sufficient force to reach the fracture limit of the infant humerus. Clinicians should apply caution in cases where such a mechanism is proposed.

Conflict of interest

ACO provides expert witness evidence to Her Majesty's courts in cases of suspected inflicted injury in children.

Acknowledgements

A.C.O. provides expert witness evidence to Her Majesty's courts in cases of suspected inflicted injury in children. This

study was supported by the Higher Committee for Education Development in Iraq (HCED). The authors would also like to acknowledge the MultiSim project (EP/K03877X/1) and CompBioMed project (H2020, grant agreement no. 675451).

References

- Hymel PK, Jenny C. Abusive spiral fractures of the humerus: a videotaped exception. *Arch Pediatr Adolesc Med* 1996;**150**:226–8 <https://doi.org/10.1001/archpedi.1996.02170270108021>.
- Somers JM, Halliday KE, Chapman S. Humeral fracture in non-ambulant infants: a possible accidental mechanism. *Pediatr Radiol* 2014;**44**(10):1219–23 <https://doi.org/10.1007/s00247-014-2954-8>.
- Rosado N. Incorrect postulate regarding humeral fractures in non-ambulant infants. *Pediatr Radiol* 2014;**44**(10):1332 <https://doi.org/10.1007/s00247-014-3124-8>.
- Jenny C. A possible mechanism for accidental humeral fractures in infants. *Pediatr Radiol* 2014;**44**(10):1218. 1218, <https://doi.org/10.1007/s00247-014-3098-6>.
- Grassi L, Schileo E, Taddei F, et al. Accuracy of finite element predictions in sideways load configurations for the proximal human femur. *J Biomech* 2012;**45**(2):394–9 <https://doi.org/10.1016/j.jbiomech.2011.10.019>.
- Lotz JC, Cheal EJ, Hayes WC. Fracture prediction for the proximal femur using finite element models: part I—linear analysis. *J Biomech Eng* 1991;**113**(4):353–60.
- Lotz JC, Hayes WC. The use of quantitative computed tomography to estimate risk of fracture of the hip from falls. *J Bone Jt Surg* 1990;**72**(5):689–700.
- Li X, Viceconti M, Cohen MC, et al. Developing CT based computational models of pediatric femurs. *J Biomech* 2015;**48**:2034–40 <https://doi.org/10.1016/j.jbiomech.2015.03.027>.
- Altai Z, Viceconti M, Offiah AC, et al. Investigating the mechanical response of paediatric bone under bending and torsion using finite element analysis. *Biomech Model Mechanobiol* 2018;**17**:1001–9 <https://doi.org/10.1007/s10237-018-1008-9>.
- Tsai A, Coats B, Kleinman PK. Biomechanics of the classic metaphyseal lesion: finite element analysis. *Pediatr Radiol* 2017;**47**(12):1622–30 <https://doi.org/10.1007/s00247-017-3921-y>.
- Meng Y, Pak W, Guleyupoglu B, et al. A finite element model of a six-year-old child for simulating pedestrian accidents. *Accid Anal Prev* 2017;**98**:206–13 <https://doi.org/10.1016/j.aap.2016.10.002>.
- Yadav P, Shefelbine SJ, Pontén E, et al. Influence of muscle groups' activation on proximal femoral growth tendency. *Biomech Model Mechanobiol* 2017;**16**(6):1869–83 <https://doi.org/10.1007/s10237-017-0925-3>.
- Schileo E, Dall'Ara E, Taddei F, et al. An accurate estimation of bone density improves the accuracy of subject-specific finite element models. *J Biomech* 2008;**41**:2483–91 <https://doi.org/10.1016/j.jbiomech.2008.05.017>.
- Zannoni C, Mantovani R, Viceconti M. Material properties assignment to finite element models of bone structures: a new method. *Med Eng Phys* 1998;**20**:735–40. 1998 [pii] <https://doi.org/S1350453398000812>.
- Taddei F, Pancanti A, Viceconti M. An improved method for the automatic mapping of computed tomography numbers onto finite element models. *Med Eng Phys* 2004;**26**:61–9 [https://doi.org/10.1016/S1350-4533\(03\)00138-3](https://doi.org/10.1016/S1350-4533(03)00138-3).
- Resnick B, editor. *Restorative care nursing for older adults: a guide for all care settings*. New York: Springer; 2004.
- Bayraktar HH, Morgan EF, Niebur GL, et al. Comparison of the elastic and yield properties of human femoral trabecular and cortical bone tissue. *J Biomech* 2004;**37**:27–35 [https://doi.org/10.1016/S0021-9290\(03\)00257-4](https://doi.org/10.1016/S0021-9290(03)00257-4).
- Warwick D, Novak G, Schultz A, et al. Maximum voluntary strengths of male adults in some lifting, pushing and pulling activities. *Ergonomics* 2007;**23**(1):49–54 <https://doi.org/10.1080/00140138008924717>.
- YouTube. <https://www.youtube.com/watch?v=bbBH5o3Lni8>. [Accessed 30 October 2018].
- YouTube. <https://www.youtube.com/watch?v=ObHsHIBLP20>. [Accessed 30 October 2018].
- Latella C, Kuppuswamy N, Romano F, et al. Whole-body human inverse dynamics with distributed micro-accelerometers, gyros and force sensing. *Sensors (Switzerland)* 2016;**16**(5):1–17 <https://doi.org/10.3390/s16050727>.
- Rajagopal A, Dembia C, DeMers M, et al. Full body musculoskeletal model for muscle-driven simulation of human gait. *IEEE Trans Biomed Eng* 2016;**63**(10):2068–79 <https://doi.org/10.1109/TBME.2016.2586891>.
- Bonnet V, Mazza C, Fraisse P, et al. Real-time estimate of body kinematics during a planar squat task using a single inertial measurement unit. *IEEE Trans Biomed Eng* 2013;**60**(7):1920–6 <https://doi.org/10.1109/TBME.2013.2245131>.
- Tamburini P, Storm F, Buckley C, et al. Moving from laboratory to real life conditions: influence on the assessment of variability and stability of gait. *Gait Posture* 2018;**59**(April 2017):248–52 <https://doi.org/10.1016/j.gaitpost.2017.10.024>.
- Bertocci GE, Pierce MC, Deemer E, et al. Using test dummy experiments to investigate pediatric injury risk in simulated short-distance falls. *Arch Pediatr Adolesc Med* 2003;**157**(5):480–6 <https://doi.org/10.1001/archpedi.157.5.480>.
- Ibrahim NG, Margulies SS. Biomechanics of the toddler head during low-height falls: an anthropomorphic dummy analysis. *J Neurosurg Pediatr* 2010;**6**(1):57–68 <https://doi.org/10.3171/2010.3.PEDS09357>.
- Sherker S, Ozanne-Smith J, Rechnitzer G, et al. Development of a multidisciplinary method to determine risk factors for arm fracture in falls from playground equipment. *Inj Prev* 2003;**9**(3):279–83 <https://doi.org/10.1136/ip.9.3.279>.